HHS Public Access

Author manuscript

Gene Ther. Author manuscript; available in PMC 2016 October 26.

Published in final edited form as:

Gene Ther. 2016 August ; 23(8-9): 680–689. doi:10.1038/gt.2016.42.

AAV-Mediated Transduction and Targeting of Retinal Bipolar Cells with Improved mGluR6 Promoters in Rodents and Primates

Q Lu[1], **TH Ganjawala**[1], **E Ivanova**[2], **JG Cheng**[3], **D Troilo**[4], and **Z-H Pan**[1,5,*]

[1]Dept. of Anatomy and Cell Biology, Wayne State University School of Medicine, Detroit, MI

[2]Burke Medical Research Institute, Weill Medical College of Cornell University, White Plains, NY

[3]Neuroscience Center, University of North Carolina, Chapel Hill, NC

[4]State University of New York, College of Optometry, New York, NY

[5]Dept. of Ophthalmology, Kresge Eye Institute, Wayne State University School of Medicine, Detroit, MI

Abstract

Adeno-associated virus (AAV) vectors have been a powerful gene delivery vehicle to the retina for basic research and gene therapy. For many of these applications, achieving cell-type specific targeting and high transduction efficiency is desired. Recently, there has been increasing interest in AAV-mediated gene targeting to specific retinal bipolar cell types. A 200-bp enhancer in combination with a basal SV40 promoter has been commonly used to target transgenes into ON-type bipolar cells. In the current study, we searched for additional cis-regulatory elements in the mGluR6 gene for improving AAV-mediated transduction efficiency into retinal bipolar cells. Our results showed that the combination of the endogenous mGluR6 promoter with additional enhancers in the introns of the mGluR6 gene markedly enhanced AAV transduction efficiency as well as made the targeting more selective for rod bipolar cells in mice. Furthermore, the AAV vectors with the improved promoter could target to ON bipolar cells with robust transduction efficiency in the para-fovea and the far peripheral retina of marmoset monkeys. The improved mGluR6 promoter constructs could provide a valuable tool for genetic manipulation in rod bipolar cells in mice and facilitate clinical applications for ON bipolar cell-based gene therapies.

[*]**Corresponding author:** Zhuo-Hua Pan, Ph.D., Department of Ophthalmology and Anatomy & Cell Biology, Wayne State University School of Medicine, 540 E. Canfield Avenue, Detroit, MI 48201, USA, zhpan@med.wayne.edu.

CONFLICT OF INTEREST

Q Lu, TH Ganjawala, JG Cheng, and Z-H Pan are inventors of the improved promoter constructs. Z-H Pan services as Scientific Advisor to RetroSense Therapeutics.

Supplementary information is available at Gene Therapy's website.

INTRODUCTION

Adeno-associated virus (AAV) vectors have been a powerful gene delivery vehicle to the retina for basic research and gene therapy[1-4]. For many of these applications, achieving cell-type specific targeting and high transduction efficiency is desired but challenging[5].

Retinal bipolar cells are comprised of multiple types that are classified into rod and cone bipolar cells based upon their synaptic inputs and ON- and OFF-types based upon their light-response polarity[6]. In mammals, there are multiple ON- and OFF-types of cone bipolar cells and a single ON-type of rod bipolar cells (RBCs). Recently, there has been increasing interest in targeted gene expression in specific retinal bipolar cell types, notably for newly emerging optogenetic gene therapy for vision restoration[7-10].

A well-known promoter for ON bipolar cell targeting is the mGluR6 promoter. A 10 kb sequence upstream of the mGluR6 gene has been shown to be sufficient to drive transgene expression in ON bipolar cells in transgenic animals[14-16]. Within the 10 kb sequence, a 200-bp mGluR6 enhancer, referred to as 200En hereinafter, was identified to be necessary for achieving ON bipolar cell targeting[14]. Most previous studies for ON bipolar cell targeting were conducted using the 200En with a basal SV40 promoter[8,14,15]; however, AAV-mediated expression with the mGluR6 promoter in retinal bipolar cells is low. Efforts have been continuously made to improve AAV-mediated gene delivery and expression efficiency to bipolar cells, especially for optogenetic gene therapy[15-17]. Factors that have been suggested to contribute to the low transduction efficiency in bipolar cells include physical barrier especially via intravitreal delivery, viral tropism, proteasome-mediated degradation, intracellular trafficking, and promoter strength[15-20].

Promoters and enhancers are key cis-regulatory elements in the regulation of gene expression[21-24]. In this study, we searched for additional regulatory elements of the mGluR6 gene for improving the AAV-mediated transduction efficiency in bipolar cells. We found that the use of the endogenous mGluR6 promoter and its intron sequences markedly enhanced the AAV-mediated transduction efficiency in RBCs in mice. For evaluating its potential clinical applications, we also examined the AAV vectors with the optimized promoter construct in a non-human primate. We showed that the AAV vectors with the improved promoter construct can target to ON bipolar cells with robust expression around the fovea and the far peripheral regions of the retina of common marmosets (*Callithrix jacchus*).

RESULTS

Bioinformatics analysis

To identify additional cis-regulatory elements of the mGluR6 gene, we conducted a bioinformatics analysis covering from a 10 kb upstream sequence through a 15 kb intrinsic sequence of the mouse mGlur6 gene (Fig. 1a). The previously identified 200-bp mGluR6 enhancer (200En; yellow box)[14] is located closed to the 5′ end of the 10 kb upstream sequence. First, a potential mGluR6 promoter sequence of 1095 bp (−1 to −1095; nucleotides relative to the translation start site), hereinafter referred to as mGluR1095P, was identified (orange arrow box) immediately upstream of the transcriptional start site of the

mGluR6 gene. Second, the binding sites for p300, an important transcription co-activator that is usually associated with promoter and enhancers[24], were marked (red circles). Within p300 dense binding regions, the binding sites for major transcription factors were identified (pink circles). Most of these transcription factors are located within intron 3, 4 and 6. Third, four conserved regions (among mouse, rat, human and dog) were identified (blue boxes or lines). The longest one largely overlaps with the 200En. Among the other conserved regions, one is located in the proximal region of the mGluR1095P and two are located in the In4.

The use of endogenous mGluR6 promoter

The optimization of the mGluR6 promoter constructs was performed in the mouse retina *in vivo* via intravitreal injection. The intravitreal route was chosen because it has the advantage of producing less retinal damage during virus injection procedures and achieving a broad homogeneous expression across the whole retina. The virus vectors were made by packaging into AAV2 serotype 2 with an Y444F capsid mutation, referred to as AAV2/2-Y444F, which has been previously reported to facilitate the transduction of retinal neurons including bipolar cells through intravitreal injection[19,20,25]. Promoter constructs containing the 200En and a varied combination of regulatory elements and promoters were evaluated by driving the transgene of mCherry (Fig. 1b).

Because the previous studies for targeting ON bipolar cells were conducted by combining the 200En with a basal SV40 promoter, 200En-SV40[8,14,15], we first examined whether the AAV-mediated transduction efficiency to ON bipolar cells could be improved by using the endogenous mGluR6 promoter. For the purpose of comparison, the AAV2-mediated expression with the promoter construct of the 200En-SV40 was tested. Consistent with these previous reports, the expression of mCherry was predominantly observed in retinal bipolar cells in retinal whole-mounts (Fig. 2a; left and middle panels) and vertical sections (Fig. 2a; right panel). At the border between inner plexiform layer (IPL) and ganglion cell layer (GCL), many axon terminals of bipolar cells were observed (Fig. 2a, middle panel). However, the expression was relatively weak (see Fig. 2g). In addition, weak expression of mCherry was frequently observed in some cells located in the inner nuclear layer (INL) and GCL after the enhancement of mCherry with antibody (see left panel in Fig. 2a; marked by arrows). The latter indicates some off targeting to retinal third order neurons.

In contrast, the transduction efficiency of the AAV vectors using the promoter construct by replacing the basal SV40 promoter with mGluR1095P was found to be markedly increased. Higher expression of mCherry was observed in retinal bipolar cells as evidenced both in retinal whole-mounts and vertical sections (Fig. 2b). The average fluorescence intensity was increased by approximately 3.7 times in comparison to the control with the 200En-SV40 promoter (Fig. 2g).

We next asked if the promoter could be shortened. A short promoter containing the 3′ 500 bp sequence (−2 to −501), referred to as mGluR500P (see Fig. 1a), was chosen based upon the presence of the p300 and a conserved region. The construct with this short promoter, 200En-mGluR500P, not only worked but also further improved transduction efficiency (Fig. 2c). The average fluorescence intensity was increased by 87% as compared to that with mGluR1095P (see Fig. 2g).

For both constructs with the mGlu1095P and mGluR500P promoter, the specificity to bipolar cells was also improved. Weak expression in other retinal neurons was only occasionally observed after the enhancement of mCherry with antibody. Thus, our results indicate that the combination of the 200En and the endogenous mGluR6 promoter can markedly increase transduction efficiency as well as improve the selectivity to bipolar cells.

Regulatory elements in the introns of mGluR6 gene

Because three introns of the mGluR6 gene contain several important transcription binding sites (see Fig. 1a), we next tested whether these introns could regulate the transduction efficiency. First, the addition of a 1130 bp sequence (4677 to 5806) of the intron 4 (referred to as In4) and a 807 bp sequence (3029 to 3835) of the intron 3 (referred to as In3) to either the 200En-mGluR1095P or the 200En-mGluR500P were found to further increase the expression level of mCherry in bipolar cells by 69% or 61% in comparison to the corresponding constructs without adding introns, respectively (Fig. 2d and e; see Fig. 2g).

Because AAV has a limited packaging capacity of 4.7 kb, we also made efforts to shorten the In3 and In4. We found that the combination of a shorten In4, In4s (690 bp; its nucleotide sequence is shown in Table S1), with the In3 further increased the average fluorescence intensity by 62% (Fig. 2f; also see Fig. 2g). Again, no significant off targeting was observed in other retinal neurons including the cells in the GCL. On the other hand, the use of a shortened In3, In3s (587 bp; see Table S1), by combining the In4s was found to decrease the expression level (data not shown). The addition of a 700 bp sequence (7457 to 8156) of the intron 6 (see Fig. 1a) to In4s-In3s-200En-mGluR500P was not found to improve the expression (data now shown), thereby suggesting that the In6 does not play a role in the regulation of mGluR6 gene expression.

As shown in Figure 2h, the transduced cell densities for the virus vectors with the improved promoter constructs were all increased compared to that with 200En-SV40 promoter, especially for the virus vectors with the promoter construct of In4s-In3-200En-mGluR500P. With the best optimized mGluR6 promoter construct, In4s-In3-200En-mGluR500P, the AAV-mediated expression could be achieved across the entire retina as a sample image shown in Figure 3a. The highest expression was usually observed in the peripheral regions of the retina.

Thus, we optimized two mGluR6 promoter constructs: a short version with 200En-mGluR500P and a longer version with In4s-In3-200En-mGluR500P. The AAV vectors with these two promoter constructs, especially the longer version, markedly increase transduction efficiency but maintain specificity to bipolar cells.

The expression was predominately in rod bipolar cells

The use of mGluR6 promoter would be expected to target the transgene to both ON cone bipolar cells and RBCs. However, the axon terminals of the mCherry expressing bipolar cells with the above optimized mGluR6 promoter constructs appeared to have the morphological characteristics of RBCs[26]; the labeled cells were stratified close to retinal ganglion cells with a few large terminal buttons. To confirm whether the targeted bipolar cells are RBCs, we performed double immunostaining with antibodies against protein kinase

C (PKC), a marker of RBCs, and mCherry[26]. Indeed, as assessed in retinal whole-mounts, 98% and 92% of the mCherry-positive bipolar cells were co-labeled with PKC for the optimized short and long mGluR6 promoter constructs respectively (Fig. 4a and c; Table 1), thereby indicating that the vast majority of them are RBCs. Only a few mCherry-positive bipolar cell terminals were observed not to be co-labeled with PKC in retinal vertical sections (Fig. 4b and d; pointed by arrows). In the best transduced regions by the virus vector with the In4s-In3-200En-mGluR500P promoter, almost all RBCs were transduced based upon PKC and mCherry co-labeling (see Fig. 4c). On average, 58% and 86% of RBCs were transduced in the peripheral retinas for the short and long mGluR6 promoter constructs, respectively (Table 1), under our conditions (with the injection of 1.5 μL virus vectors at the titer of 1×10^{13} vg/mL).

To address whether the predominant targeting to RBCs is due to the property of the endogenous mGluR6 promoter, we performed co-labeling of PKC and mCherry in the retina that was transduced by the virus vectors with the 200En-SV40 promoter. The majority of the transduced cells were also RBCs although mCherry-positive but PKC negative bipolar cells were frequently observed (Figure S1). Our results thus suggest the virus vectors with the 200En-SV40 promoter also preferably target RBCs but the virus vectors with the endogenous mGluR6 promoter appear to be more selective to RBCs.

Since a new AAV2 capsid variant, named 7m8, developed through *in vivo*-directed evolution in the mouse retina, was recently reported to be able to improve transduction efficiency via intravitreal injection both in the mouse and primate retinas[27], we therefore also produced the virus vector for the promoter construct of In4s-In3-200En-mGluR500P with the 7m8 capsid plus Y444F mutation, referred to as AAV2.7m8-Y444F hereinafter. Its expression was first examined in the mouse retina. Consistently, the overall expression was improved as evidenced by the increase of the mCherry-positive bipolar cells in retinal whole-mounts (Fig. 3b and 5a). Quantitatively, a higher percentage of PKC-positive cells (96%) was co-labeled with mCherry (Table 1). However, the percentage (86%) of PKC and mCherry co-labeled cells in the mCherry-positive bipolar cells was decreased comparing to that of the virus vector with the AAV2/2-Y444F capsid, suggesting that other bipolar cells other than RBCs were transduced. Indeed, in retinal vertical sections, more PKC-negative and mCherry-positive bipolar cells were observed (Fig. 5b-d). Most of these PKC-negative bipolar cells were co-labeled with antibody against $G\gamma_{13}$, a marker of both ON cone bipolar cells and RBCs[28] (Fig. 5e-g; pointed by arrows in Fig. 5g), indicating that they are mainly ON cone bipolar cells. Additionally, more weakly transduced RGCs or amacrine cells were observed (pointed by arrow heads in Fig. 5g). Together, these results indicate that the virus vector with the AAV2.7m8-Y444F capsid improves the transduction efficiency but is slightly less selective to RBCs compared to that of the virus vector with the AAV2/2-Y444F capsid in the mouse retina.

AAV-mediated expression in the marmoset retina

To begin evaluating its potential clinical applications, we examined the AAV-mediated specificity and transduction efficiency in the marmoset retina using virus vectors with the In4s-In3-200En-mGluR500P promoter packaged by both AAV2/2-Y444 and AAV2.7m8-

Y444F capsids. The virus vectors were administered via intravitreal injection in four eyes of four animals, three eyes were injected with the AAV2/2-Y444F capsid and one eye was injected with the AAV2.7m8-Y444F capsid. As shown in Fig. 6a and b, for both virus vectors, the expression of mCherry was observed in the regions surrounding the fovea (labeled as 1; also pointed by arrows), the far peripheral retinas (labeled as 2) first occurring ~5 – 6 mm away from the fovea, and along retinal blood vessels (labeled as 3; the insertions show the high magnification for the labeled areas). The expression was more robust with the vectors carrying the AAV2.7m8-Y444F capsid (also see Table 2). At a higher magnification, the mCherry-positive cells with the morphological appearance of bipolar cells formed a dense ring surrounding the center of the fovea (Fig. 6c and d). The highest transduction efficiency was observed in the far peripheral regions of the retina.

To determine the transduced bipolar cell types, we performed triple immunolabeling in retinal whole-mounts in the peripheral retina of 6 – 8 mm away from the fovea with antibodies against mCherry, PKC, and $G\gamma_{13}$. For the virus vector with the AAV2.7m8-Y444F capsid, 95% of the mCherry-positive bipolar cells were co-labeled with $G\gamma_{13}$ (Fig. 7a-c; Table 2), indicating that the vast majority of the transduced bipolar cells were ON bipolar cells. PKC co-labeling indicated that only 17% of the transduced bipolar cells were RBCs (Fig. 7d-f; Table 2). Based upon the co-labeling of PKC and $G\gamma_{13}$ in the examined regions, 24 – 25% of the ON bipolar cells were RBCs (see Table 2), consistent with the previously reports that only a small portion of the ON bipolar cells is RBCs in the marmoset retina[29,30]. The vast majority (93%) of the $G\gamma_{13}$-positive cells (ON bipolar cells), and the majority (72%) of the PKC-positive cells (RBCs) were transduced (see Table 2). Together, these results indicate that in the peripheral marmoset retina the virus vector with AAV2.7m8-Y444F capsid can efficiently target the majority of the ON cone bipolar cells and RBCs with high transduction efficiency. This was also confirmed by double-labeling of mCherry with $G\gamma_{13}$ or PKC in retinal vertical sections. The mCherry-positive cells were almost all co-labeled with $G\gamma_{13}$ (Fig. 8a). mCherry-positive, but $G\gamma_{13}$-negative bipolar cells were only occasionally observed. Additionally, the vast majority of $G\gamma_{13}$-positive and the majority of PKC-positive cells were co-labeled with mCherry (Fig. 8a and b).

For the virus vector with AAV2/2-Y444F capsid, the specificity is similar to that of the virus vector with AAV2.7m8-Y444F capsid (Figure S2). That is, the virus vectors were observed to predominantly target both ON cone bipolar cells and RBCs, however the overall transduction efficiency is reduced (Table 2).

Discussion

In this study, we have improved the mGluR6 promoter constructs for AAV-mediated retinal bipolar cell targeting via intravitreal administration in the mouse retina. The AAV vectors with the best optimal promoter construct, In4s-In3-200En-mGluR500P, increased the expression level by over 20x in comparison to that of the 200En-SV40 promoter. The maximal genome that could be packaged into AAV vectors is ~4.7 kb[31]. The In4s-In3-200En-mGluR500P construct is approximately 2.2 kb in length; so for AAV-mediated expression, it can still hold a transgene of up to 2.0 kb, assuming the use of a 0.5 kb poly(A) sequence. For longer transgenes, the short version of the mGluR6 promoter construct,

200En-mGluR500P, could be used, which can hold a transgene of up to 3.5 kb. In addition, the optimized promoter construct also reduced off-targeting to other retinal neurons.

The increase in the transduction efficiency was achieved by using the endogenous mGluR6 promoter and by incorporating the mGluR6 gene introns. Our results indicate that the endogenous mGluR6 promoter is more effective than the basal SV40 promoter. In addition, our results indicate the presence of the additional enhancers in the introns of 3 and 4 of mGluR6 gene. Interestingly, the shortened mGluR6 promoter and the shortened In4 were found to be more effective than the long versions. The latter suggests the presence of suppressors in these sequences[23]. It may be possible to further improve the transduction efficiency by fine-tuning these sequences or by searching for additional regulatory elements.

Our results show that the use of endogenous mGluR6 promoter also results in the improvement of the selectivity to bipolar cells. This is important because an increase of the transduction efficiency is usually associated with an increase in off-targeting. Interestingly, in the mouse retina, the promoter constructs with the endogenous mGluR6 promoter were found to predominantly target to RBCs. Our results indicate that the 200En-SV40 construct also preferably targeted to RBCs, suggesting that this property is in part due to the property of the 200En. However, the use of the endogenous mGluR6 promoter appeared to make the virus vectors more selective to RBCs. Because the 10 kb sequence upstream to the translation start site was shown to be capable of targeting to all ON bipolar cells[11-13], it is possible that there is additional regulatory element(s) within the 10 kb sequence that may regulate the transgene expression in ON cone bipolar cells. Further studies would be interesting to search such regulatory elements.

It should be noted that in addition to the commonly used 200En-SV40 promoter, an enhanced mGluR6-based promoter containing multiple 200Ens, 4 × 200En, was used to improve the transduction efficiency to ON bipolar cells in the mouse retina[16]. A bipolar cell selective MiniPromoter was also reported to target ON bipolar cells in the mouse retina[32,33]. However, since different AAV capsids and variants were used in these studies, a comparison side-by-side would be required to determine the selectivity and transduction efficiency of the constructs developed in this study over these previously reported promoters.

Nevertheless, the predominant selectivity of our improved constructs for RBCs will offer a valuable tool for genetic manipulation in RBCs in the mouse model. Due to the low transduction efficiency and the lack of high selectivity of virus mediated delivery in general, cell-type specific targeted genetic manipulation was commonly achieved by using transgenic lines, especially Cre lines. However, creating transgenic mouse lines is both costly and time consuming. In fact, no highly RBC-selective Cre mouse lines are currently available[20]. Thus, with the improved targeting selectivity and transduction efficient for RBCs, the AAV-mediated gene delivery would be a more feasible and cost efficient approach for introducing Cre or transgenes directly in RBCs in the mouse retina. This approach would be particularly advantageous for cell targeting in species in which the transgenic strategy is not applicable.

Our results show that the AAV vectors with the optimized promoter construct can selectively target bipolar cells in the marmoset retina with intravitreal injection. Robust transduction

efficiency can be achieved in the regions surrounding the fovea and in the far peripheral retina. The vast majority of the ON bipolar cells in the far peripheral retina could be transduced, indicating the promoter construct is highly effective in the primate.

Interestingly, in contrast to the results observed in the mouse retina, the AAV vectors with the optimized mGluR6 promoter construct in the marmoset retina were found to transduce not only RBCs but also ON cone bipolar cells. This species difference could not be explained by the difference in the ratios of RBCs versus ON cone bipolar cells between these two species. In the mouse retina, the majority of the transduced bipolar cells (92% and 82% for the virus vectors with AAV2/2-Y444F and AAV2/7m8-Y444F capsid, respectively; Table 1) are RBCs. The ratio of RBCs and ON cone bipolar cells was reported to be ~1.3:1[34]. The density of our counted RBCs (10,000 – 11,000/mm^2; see Table 1) is close to the low end of the previously reported range (11,000 – 15,000/mm^2)[34,35]. In contrast, in the marmoset retina, only 17 – 18% of the transduced bipolar cells are RBCs. The ratio of RBCs and ON cone bipolar cells based on our counting is about 1:4 in the examined far peripheral region (6 – 8 mm away from the fovea) (see Table 2). As a note, this ratio appears to be higher than that previously reported (1 or 3 mm away from the fovea)[29,30], which could be overestimated under our conditions, possibly due to the weak labeling of some types of ON bipolar cells with Gγ_{13}. The latter may suggest that there is no preferable transduction in RBCs in the marmoset retina. Together, our results clearly indicate that the virus vectors predominately target RBCs in the mouse retina but target both RBCs and ON cone bipolar cells in the marmoset retina.

The difference in targeting between mice and marmosets could be due to a different transcriptional regulation between these two species. Further studies of the differences in the transcription binding sites between the mouse and marmoset could be performed to determine the regulatory components for RBCs and ON cone bipolar cells. Nevertheless, the ability of the optimized mGluR6 promoter construct to target all ON bipolar cells by AAV vectors offers an effective promoter for ON bipolar cell targeting in the marmosets.

To our knowledge, this study is the first to demonstrate the ability of AAV-mediated expression of targeting retinal bipolar cells in non-human primates. The marmoset has become increasing popular as a non-human primate model for gene therapy[36-39] and eye and vision research because the anatomical properties of the marmoset eye and retina are similar to those of humans[40-44]. Thus, the improved mGluR6 promoter constructs developed in this study could facilitate pre-clinical testing and applications for the ON bipolar cell-based gene therapies, especially optogenetic gene therapy for vision restoration[9,10, 45-47].

Our results showed that the transduction efficiency in the marmoset retinas was varied in different retinal regions. The transduction efficiency was very low or none beyond the regions of the para-fovea and the far peripheral retina, excepting around blood vessels. A similar expression pattern was previously reported by AAV vectors with strong ubiquitous promoters, e.g., CAG and CMV, which non-selectively transduced inner retinal neuron in the marmoset[38] and the macaque retina[27,48]. Such uneven transduction efficiency may be due to the presence of certain retinal barriers, mainly the inner limiting membrane[18,38].

Our results also showed that AAV vectors that use AAV2.7m8 capsid variant resulted in a marked increase in the overall expression both in mice and marmosets. An increase of transduction efficiency in bipolar cells in mice using the AAV2.7m8 capsid was recently reported using the 200En-SV40 promoter[17]. This was proposed to be due to improvement of the overall virus penetration in the retina[27]. Thus further improving the virus penetration in the primate retinas is needed. This could be achieved by the combination of optimizing capsid variants, enzymatic treatments, or surgery to remove the inner limiting membrane to facilitate the virus penetration in the primate retina[18,48]. Further improvement of the transduction efficiency in primates could also be achieved by including additional capsid mutations to reduce proteasome-mediated degradation[49,50].

MATERIALS AND METHODS

Bioimformatics analysis

Using Ensembl genome browser (www.ensembl.org), mouse mGlurR6 (Grm6) gene sequence of 25 kb was downloaded from the National Institutes of Health (NIH) gene database (GenBank accession number NC_000077.6). Cis-RED (Nucleic Acid Research; http://www.cisred.org/) and Promoter Scan (http://www-bimas.cit.nih.gov/molbio/proscan/) programs were used to define the proximal promoter of mGluR6. The transcriptional binding site analysis program (TFSEARCH; Parallel Application TRC Laboratory, RWCP, Japan) and the Ensembl genome browser (www.ensembl.org) were used to mark the p300 binding site, an important transcription co-activator, and search specific transcriptional factor binding sites. For selection of potential regulatory elements, preference was given to conserved DNA sequences and the region with dense p300 binding sites.

Virus vector constructs and virus vectors

A series of AAV2 expression cassettes were constructed to contain the 200En and a variety of the combinations of potential regulatory elements and promoters of the mGluR6 gene to drive the transgene of mCherry. The DNAs of the mGluR6 regulatory sequences were synthesized (Genescript, Piscataway, NJ, USA). All virus vectors in the mouse experiments were made by packaging into serotype 2 with an Y444F capsid mutation. The virus vectors for the marmoset experiments were also made by packaging into AAV2.7m8 capsid construct with the addition of the Y444F capsid mutation. The AAV2.7m8 capsid construct was kindly provided by John Flannery at UC Berkeley. The Y444F capsid mutation was introduced by site-directed mutagenesis (Agilent Technologies, Santa Clara, CA, USA). Viral vectors were packaged and affinity purified by Virovek (Hayward, CA, USA).

Animals and virus injection

C57BL/6J mice of either sex were purchased from Jackson Laboratory (Bar Harbor, ME, USA). The marmosets were bred and housed at the State University of New York (SUNY) College of Optometry. The mouse-related experiments and procedures were approved by the Institutional Animal Care and Use Committee (IACUC) at Wayne State University and the marmoset-related experiments and procedures were approved by the IACUC at SUNY College of Optometry. All animal use in this study was in accordance with the NIH Guide for the Care and Use of Laboratory Animals.

Virus injections were performed in mice at the age of about one month. The mouse was anesthetized by intraperitoneal injection of a mixture of 120 mg/kg ketamine and 15 mg/kg xylazine. Under a dissecting microscope, a small perforation was made in the temporal sclera region with a sharp needle. A total of 1.5 μL of viral vectors suspension in saline at a concentration of ~1×10^{13} vg/mL was injected into the intravitreal space through the perforation with 32-gauge blunt Hamilton syringe. The expression was examined about one month after the viral injection.

Virus injections were performed in four juvenile female marmosets at the age of 6 - 9 months. The animals were anesthetized by intramuscular injection of alfaxalone (2 mg/100 g body weight). A total of 30 μL of virus vectors suspension in saline at a concentration of ~1×10^{13} vg/mL was injected into the intravitreal space with a 0.5-mL syringe with a 32-gauge sharp-point needle. The injection site was chosen on the temporal side of the eyeball, 2 mm posterior to the limbus. The animals were given an analgesic NSAID (carprofen, 5–10 mg/kg SC) after surgery. The expression was examined one to two months after the viral injection.

Immunohistochemistry

Mice were euthanized by CO_2 asphyxiation followed by decapitation. Marmosets were anesthetized with alfaxalone (2 mg/100 g body weight) and euthanatized by an intracardiac injection of pentobarbital. The retinas were fixed in 4% paraformaldehyde in phosphate buffer (PB) for 20 minutes.

In the mouse retina, for quantitative comparison of the expression level of mCherry, the fluorescence images were directly taken from the fixed retinas without immunostaining. The fixed retinas were dissected in PB solution, flat mounted on slides, and coverslipped after adding with mounting medium.

For immunostaining of whole-mount retinas, the retinas were incubated for 2 hrs in a block solution containing 5% ChemiBLOCK (Millipore Corp., Bedford, MA, USA), 0.5% Triton X-100 and 0.05% sodium azide (Sigma-Aldrich, St. Louis, MO, USA). The primary antibodies were diluted in the same solution and applied for two days for mouse retinas and seven days for marmoset retinas at room temperature (RT). The retinas were then washed several times, followed by incubation in the secondary antibodies for one day for mouse retina and five days for marmoset retinas in RT.

For immunostaining of retinal vertical sections, the retinas were cryoprotected in graded sucrose (10%, 20%, and 30% wt/vol, respectively, in PB) and cut at 20 μm. The retinal sections were incubated for 1 hr in the block solution. The primary antibodies were diluted in the same solution and applied overnight in RT, followed by incubation of 2 hrs in the secondary antibodies. The secondary antibodies were conjugated to Alexa 594 (1:1000), or Alexa 555 (1:1000), or Alexa 488 (1:600; Thermo Fisher Scientific, Waltham, MA, USA), or AMCA (1:200; JacksonImmunoResearch, West Grove, PA, USA). The following primary antibodies were used in this study: rabbit anti-mCherry (1:500; Clontech, Mountain View, CA, USA); goat anti-mCherry (1:2000; Biorbyt, Cambridge, UK); rabbit anti-PKC

(1:20,000; Cell Signal, Danvers, MA, USA), mouse anti-PKC (1:10000; Santa Cruz, Dallas, Texas, USA), rabbit anti-Gγ13 (1:1000; Santa Cruz).

All images were acquired using a Zeiss Axio Imager 2 microscope with an Apotome 2 oscillating grating to reduce out-of-focus stray light (Apotome; Carl Zeiss Microscopy GmbH, Jena, Germany). Image projections were constructed by collapsing individual z-stacks of optical sections onto a single plane in ZEN software (Carl Zeiss). The brightness and the contrast were adjusted using Adobe Photoshop (Photoshop CS4; Adobe Systems, San Jose, CA).

Quantitative fluorescence and cell density measurements

All quantifications for fluorescent intensity and cell density were performed using ImageJ software (NIH). In mice, each virus construct was injected in both eyes of 4 – 6 animals. Good transgene expression that exhibited relatively even expression across the retina could be achieved in about half of the injected eyes. Therefore, randomization or blinding methods were not used for comparison. Instead, the best transduced retinas (2 – 3 retinas for each construct) were chosen for the analysis. The images were taken from whole-mounts without antibody enhancement. In each retina, 6 - 12 images were taken from the peripheral regions (~2 mm from the optic disc) with the same fixed exposure time. The fluorescence intensity was calculated based upon a method previously described[47]. The “Image – Adjust – Threshold” function of the software was used to select the cells. The “Analyze – Analyze particles” function was used to obtain the cell number and the total fluorescence intensity of each cell (the sum of the fluorescence values of all pixels within a cell). The average fluorescence intensity for each cell was calculated with the following formula: total intensity of the cell/the area of the cell - background signal, where background signal = average signal for a region without cells. Overlapped cells could be counted as a single cell by the software, so all sections were inspected and cell counts were corrected manually. The fluorescence intensity was presented as the mean ± SD of the average fluorescence intensity of all measured cells. In marmosets, the double and triple immunostaining and cell counting were performed in the periphery retina 6 – 8 mm away from the fovea.

Supplementary Material

Refer to Web version on PubMed Central for supplementary material.

ACKNOWLEDGEMENTS

This work was supported by National Institutes of Health (NIH) grant EY17130 (ZHP), core grant EY04068 to Department of Anatomy and Cell Biology at Wayne State University, Dryer Foundation, the Ligon Research Center of Vision, and Research to Prevent Blindness to Department of Ophthalmology at Wayne State University.

REFERENCES

1. Zhu Y, Xu J, Hauswirth WW, DeVries SH. Genetically targeted binary labeling of retinal neurons. J Neurosci. 2014; 34:7845–7861. [PubMed: 24899708]
2. Maguire AM, Simonelli F, Pierce EA, Pugh EN Jr, Mingozzi F, Bennicelli J, et al. Safety and efficacy of **gene** transfer for Leber's congenital amaurosis. N Engl J Med. 2008; 358:2240–2248. [PubMed: 18441370]

3. Boye SE, Boye SL, Lewin AS, Hauswirth WW. A comprehensive review of retinal gene therapy. Mol. Ther. 2013; 21:509–519. [PubMed: 23358189]
4. Trapani I, Puppo A, Auricchio A. Vector platforms for gene therapy of inherited retinopathies. Prog Retin Eye Res. 2014; 43:108–128. [PubMed: 25124745]
5. Vandenberghe LH, Auricchio A. Novel adeno-associated viral vectors for retinal gene therapy. Gene Ther. 2012; 19:162–168. [PubMed: 21993172]
6. Euler T, Haverkamp S, Schubert T, Baden T. Retinal bipolar cells: elementary building blocks of vision. Nat Rev Neurosci. 2014; 15:507–519. [PubMed: 25158357]
7. Bi A, Cui J, Ma YP, Olshevskaya E, Pu M, Dizhoor AM, et al. Ectopic expression of a microbial-type rhodopsin restores visual responses in mice with photoreceptor degeneration. Neuron. 2006; 50:23–33. [PubMed: 16600853]
8. Lagali PS, Balya D, Awatramani GB, Munch TA, Kim DS, Busskamp V, et al. Light-activated channels targeted to ON bipolar cells restore visual function in retinal degeneration. Nat Neurosci. 2008; 11:667–675. [PubMed: 18432197]
9. Busskamp V, Picaud S, Sahel JA, Roska B. Optogenetic therapy for retinitis pigmentosa. Gene Ther. 2012; 19:169–175. [PubMed: 21993174]
10. Pan Z-H, Lu Q, Bi A, Dizhoor AM, Abrams GW. Optogenetic Approaches to Restoring Vision. Annu Rev Vis Sci. 2015; 1:185–210.
11. Ueda Y, Iwakabe H, Masu M, Suzuki M, Nakanishi S. The mGluR6 5′ upstream transgene sequence directs a cell-specific and developmentally regulated expression in retinal rod and ON-type cone bipolar cells. J Neurosci. 1997; 17:3014–3023. (1997). [PubMed: 9096137]
12. Morgan JL, Dhingra A, Vardi N, Wong RO. Axons and dendrites originate from neuroepithelial-like processes of retinal bipolar cells. Nat Neurosci. 2006; 9:85–92. [PubMed: 16341211]
13. Dhingra A, Sulaiman P, Xu Y, Fina ME, Veh RW, Vardi N. Probing neurochemical structure and function of retinal ON bipolar cells with a transgenic mouse. J Comp Neurol. 2008; 510:484–496. [PubMed: 18671302]
14. Kim DS, Matsuda T, Cepko CL. A core paired-type and POU homeodomain-containing transcription factor program drives retinal bipolar cell gene expression. J Neurosci. 2008; 28:7748–7764. 2008. [PubMed: 18667607]
15. Doroudchi MM, Greenberg KP, Liu J, Silka KA, Boyden ES, Lockridge JA, et al. Virally delivered channelrhodopsin-2 safely and effectively restores visual function in multiple mouse models of blindness. Mol Ther. 2011; 19:1220–1229. [PubMed: 21505421]
16. Cronin T, Vandenberghe LH, Hantz P, Juttner J, Reimann A, Kacsó AE, et al. Efficient transduction and optogenetic stimulation of retinal bipolar cells by a synthetic adeno-associated virus capsid and promoter. EMBO Mol Med. 2014; 6:1175–1190. [PubMed: 25092770]
17. Mace E, Caplette R, Marre O, Sengupta A, Chaffiol A, Barbe P, et al. Targeting channelrhodopsin-2 to ON-bipolar cells with vitreally administered AAV restores ON and OFF visual responses in blind mice. Mol Ther. 2015; 23:7–16. [PubMed: 25095892]
18. Dalkara D, Kolstad KD, Caporale N, Visel M, Klimczak RR, Schaffer DV, et al. Inner limiting membrane barriers to AAV-mediated retinal transduction from the vitreous. Mol Ther. 2009; 17:2096–2102. [PubMed: 19672248]
19. Petrs-Silva H, Dinculescu A, Li Q, Deng WT, Pang JJ, Min SH, et al. Novel properties of tyrosine-mutant AAV2 vectors in the mouse retina. Mol Ther. 2011; 19:293–301. [PubMed: 21045809]
20. Lu Q, Ivanova E, Ganjawala HT, Pan Z-H. Cre-mediated recombination efficiency and transgene expression patterns of three retinal bipolar cell-expressing Cre transgenic mouse lines. Mol Vis. 2013; 19:1310–1320. [PubMed: 23805038]
21. Butler JE, Kadonaga JT. The RNA polymerase II core promoter: a key component in the regulation of gene expression. Genes Dev. 2002; 16:2583–2592. [PubMed: 12381658]
22. Papadakis ED, Nicklin SA, Baker AH, White SJ. Promoters and control elements: designing expression cassettes for gene therapy. Curr Gene Ther. 2004; 4:89–113. [PubMed: 15032617]
23. Pennacchio LA, Bickmore W, Dean A, Nobrega MA, Bejerano G. Enhancers: five essential questions. Nat Rev Genet. 2013; 14:288–295. [PubMed: 23503198]
24. Visel A, Blow MJ, Li Z, Zhang T, Akiyama JA, Holt A, Plajzer-Frick I, et al. ChIP-seq accurately predicts tissue-specific activity of enhancers. Nature. 2009; 457:854–858. [PubMed: 19212405]

25. Petrs-Silva H, Dinculescu A, Li Q, Min SH, Chiodo V, Pang JJ, et al. High-efficiency transduction of the mouse retina by tyrosine-mutant AAV serotype vectors. Mol Ther. 2009; 17:463–471. [PubMed: 19066593]
26. Greferath U, Grünert U, Wässle H. Rod bipolar cells in the mammalian retina show protein kinase C-like immunoreactivity. J Comp Neurol. 1990; 301:433–442. [PubMed: 2262600]
27. Dalkara D, Byrne LC, Klimczak RR, Visel M, Yin L, Merigan WH, et al. In vivo-directed evolution of a new adeno-associated virus for therapeutic outer retinal gene delivery from the vitreous. Sci Transl Med. 2013; 5:189ra76.
28. Huang L, Max M, Margolskee RF, Su H, Masland RH, Euler T. G protein subunit Gγ13 is coexpressed with Gαo, Gβ3, and Gβ4 in retinal ON bipolar cells. J Comp Neurol. 2003; 455:1–10. [PubMed: 12454992]
29. Chan TL, Martin PR, Clunas N, Grünert U. Bipolar cell diversity in the primate retina: morphologic and immunocytochemical analysis of a new world monkey, the marmoset Callithrix jacchus. J Comp Neurol. 2001; 437:219–239. [PubMed: 11494253]
30. Weltzien F, Percival KA, Martin PR, Grünert U. Analysis of bipolar and amacrine populations in marmoset retina. J Comp Neurol. 2015; 523:313–334. [PubMed: 25262625]
31. Surace EM, Auricchio A. Versatility of AAV vectors for retinal gene transfer. Vis Res. 2008; 48:353–359. [PubMed: 17923143]
32. de Leeuw CN, Dyka FM, Boye SL, Laprise S, Zhou M, Chou AY, et al. Targeted CNS Delivery Using Human MiniPromoters and Demonstrated Compatibility with Adeno-Associated Viral Vectors. Mol Ther Methods Clin Dev. 2014; 1:5. [PubMed: 24761428]
33. Scalabrino ML, Boye SL, Fransen KM, Noel JM, Dyka FM, Min SH, et al. Intravitreal delivery of a novel AAV vector targets ON bipolar cells and restores visual function in a mouse model of complete congenital stationary night blindness. Hum Mol Genet. 2015; 24:6229–6239. [PubMed: 26310623]
34. Wässle H, Puller C, Müller F, Haverkamp S. Cone contacts, mosaics, and territories of bipolar cells in the mouse retina. J Neurosci. 2009; 29:106–117. [PubMed: 19129389]
35. Strettoi E, Pignatelli V. Modifications of retinal neurons in a mouse model of retinitis pigmentosa. Proc Natl Acad Sci USA. 2000; 97:11020–11025. [PubMed: 10995468]
36. Hibino H, Tani K, Ikebuchi K, Wu MS, Sugiyama H, Nakazaki Y, et al. The common marmoset as a target preclinical primate model for cytokine and gene therapy studies. Blood. 1999; 93:2839–2848. [PubMed: 10216078]
37. t'Hart BA, Vervoordeldonk M, Heeney JL, Tak PP. Gene therapy in nonhuman primate models of human autoimmune disease. Gene Ther. 2003; 10:890–901. [PubMed: 12732874]
38. Ivanova E, Hwang GS, Pan ZH, Troilo D. Evaluation of AAV-mediated expression of Chop2-GFP in the marmoset retina. Investig Ophthalmol Vis Sci. 2010; 51:5288–5296. 2010. [PubMed: 20484599]
39. Baba Y, Satoh S, Otsu M, Sasaki E, Okada T, Watanabe S. In vitro cell subtype-specific transduction of adeno-associated virus in mouse and marmoset retinal explant culture. Biochimie. 2012; 94:2716–2822. [PubMed: 22971462]
40. Troilo D, Howland HC, Judge SJ. Visual optics and retinal cone topography in the common marmoset (*Callithrix jacchus*). Vision Res. 1993; 33:1301–1310. [PubMed: 8333154]
41. Goodchild AK, Ghosh KK, Martin PR. Comparison of photoreceptor spatial density and ganglion cell morphology in the retina of human, macaque monkey, cat, and the marmoset Callithrix jacchus. J Comp Neurol. 1996; 366:55–75. [PubMed: 8866846]
42. Wilder HD, Grunert U, Lee BB, et al. Topography of ganglion cells and photoreceptors in the retina of a New World monkey: the marmoset Callithrix jacchus. Vis Neurosci. 1996; 13:335–352. [PubMed: 8737285]
43. Hendrickson A, Troilo D, Djajadi H, Possin D, Springer A. Expression of synaptic and phototransduction markers during photoreceptor development in the marmoset monkey Callithrix jacchus. J Comp Neurol. 2009; 512:218–231. [PubMed: 19003975]
44. Hendrickson A, Troilo D, Possin D, Springer A. Development of the neural retina and its vasculature in the marmoset Callithrix jacchus. J Comp Neurol. 2006; 497:270–286. [PubMed: 16705674]

45. Cehajic-Kapetanovic J, Eleftheriou C, Allen AE, Milosavljevic N, Pienaar A, Bedford R, et al. Restoration of Vision with Ectopic Expression of Human Rod Opsin. Curr Biol. 2015; 25:2111–2122. [PubMed: 26234216]

46. Gaub BM, Berry MH, Holt AE, Reiner A, Kienzler MA, Dolgova N, et al. Restoration of visual function by expression of a light-gated mammalian ion channel in retinal ganglion cells or ON-bipolar cells. PNAS. 2014; 111:E5574–5583. [PubMed: 25489083]

47. Gaub BM, Berry MH, Holt AE, Isacoff EY, Flannery JG. Optogenetic Vision Restoration Using Rhodopsin for Enhanced Sensitivity. Mol Ther. 2015; 23:1562–1571. [PubMed: 26137852]

48. Yin L, Greenberg K, Hunter JJ, Dalkara D, Kolstad KD, Masella BD, et al. Intravitreal injection of AAV2 transduces macaque inner retina. Investig Ophthalmol Vis Sci. 2011; 52:2775–2783. 2011. [PubMed: 21310920]

49. Kay CN, Ryals RC, Aslanidi GV, Min SH, Ruan Q, Sun J, et al. Targeting photoreceptors via intravitreal delivery using novel, capsid-mutated AAV vectors. Plos One. 2013; 8:e62097. [PubMed: 23637972]

50. Aslanidi GV, Rivers AE, Ortiz L, Song L, Ling C, Govindasamy L, et al. Optimization of the capsid of recombinant adeno-associated virus 2 (AAV2) vectors: the final threshold? PLoS One. 2013; 8:e59142. [PubMed: 23527116]

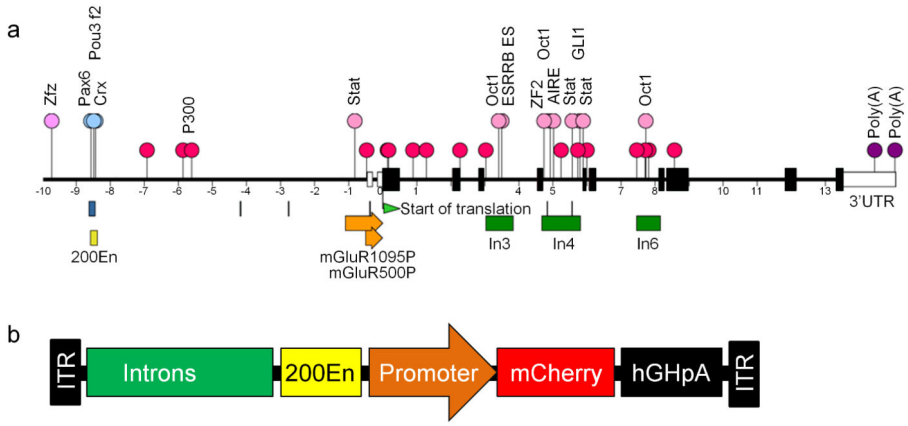

Figure 1. Bioinformatics analysis of mGluR6 gene and AAV virus cassette

(**a**) A schematic diagram of the 25 kb sequence associated with the mGluR6 gene with the 10 kb upstream sequence of a translation start site (green arrow) and the 15 kb intrinsic sequence. The two white boxes preceding the translation start site are non-coding sequence (5′ UTR). The ATG (nucleotide 1 – 3) containing an exon was assigned as exon 1 followed by other axons (black boxes). The p300 binding sites and the potential important transcriptional binding sits are marked as red and pink circles, respectively. Blue squares and lines are conserved regions. The 1095 bp and 500 bp mGluR6 promoters are shown as orange arrows. The sequences of the intron 3, 4 and 6 (In3, In4, and In6) are shown as green boxes. The previous identified 200 enhancer (200En) is shown as a yellow box. The poly(A) sites (purple circles) within the 3′ untranslated region (3'UTR; while box) are labeled. Three previously reported transcriptional binding sites within the 200En are labeled as blue circles[14]. (**b**) The schematic diagram of AAV cassettes which contain 200En with or without preceding intron(s) and followed by a promoter to drive the transgene of mCherry with a human growth hormone poly(A).

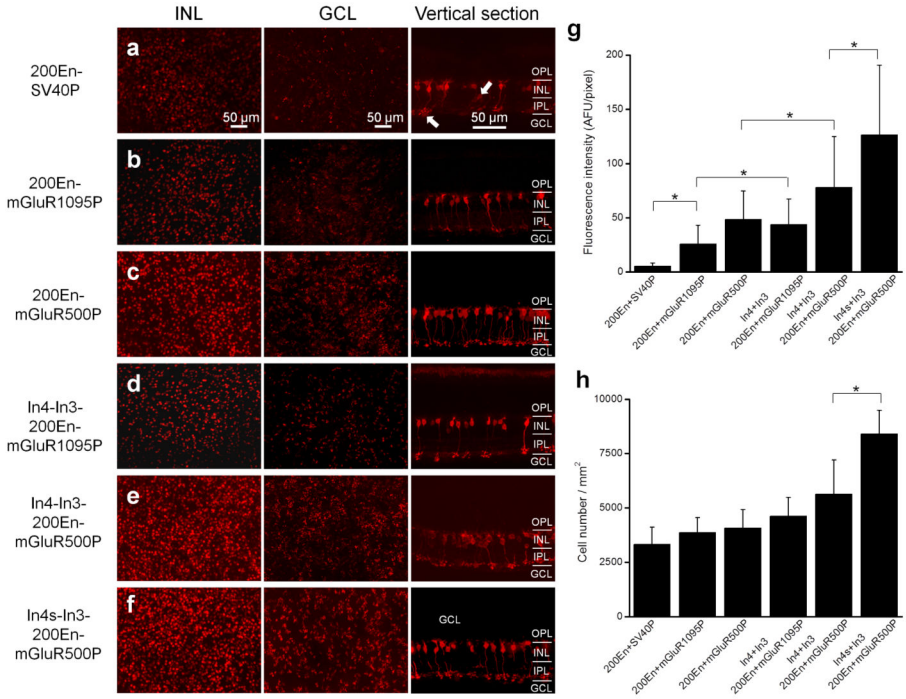

Figure 2. Comparison of the AAV-mediated transduction efficiency in the mouse retinas with different mGluR6 promoter constructs

(**a – f**) The left and middle panels show the whole-mount fluorescence images acquired with the focal plan at the inner nuclear layer (left panels) and ganglion cell layer (middle panels) without immunolabeling. The right panels show the vertical section images after immunolabeling with mCherry. The arrows point to mCherry-expressing ganglion cells or amacrine cells. (**g)** Comparison of the fluorescence intensities of the mCherry-expressing bipolar cells with different mGluR6 promoter constructs. (**h**) Comparison of the cell densities of the mCherry-expressing bipolar cells with different mGluR6 promoter constructs. The cell density counts were restricted to cells in the inner nuclear layer. The data are shown as the mean ± SD. The asterisk indicates statistically significant differences at $p < 0.05$ (one-way ANOVA). OPL: outer plexiform layer; INL: inner nuclear layer; IPL: inner plexiform layer; GCL: ganglion cell layer.

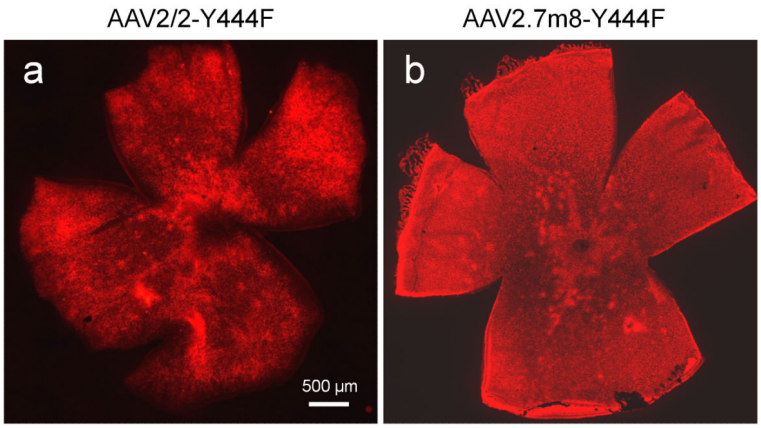

Figure 3. AAV-mediated expression of mCherry in retinal whole mounts in mice

The images of the retina whole-mount injected with the virus vector carrying the promoter In4s-In3-200En-mGluR500P with AAV2/2-Y444F (**a**) and AAV2.7m8-Y444F (**b**) capsid variants.

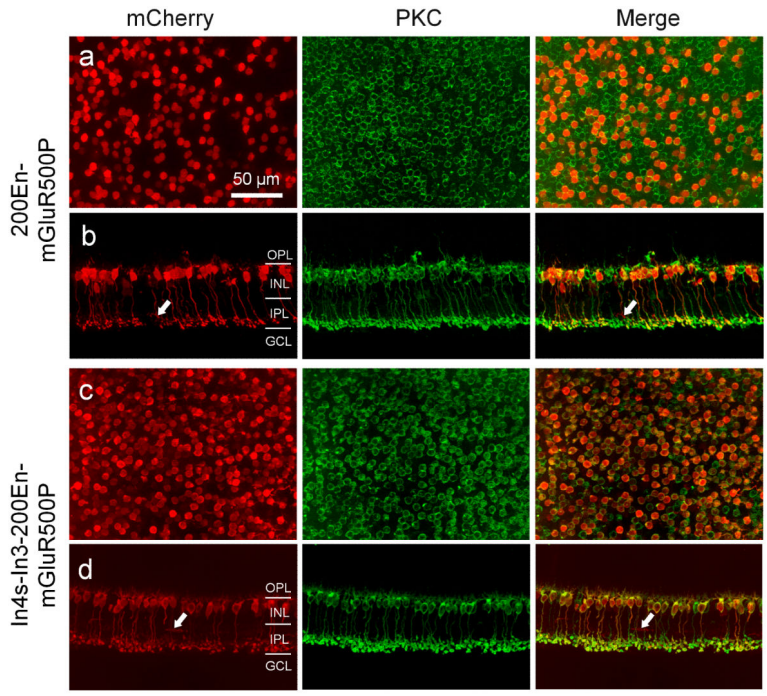

Figure 4. Immunostaining for the characterization of mCherry-expressing bipolar cells transduced by the virus vectors with AAV2/2-Y444F capsid variant in mice

The expression of mCherry was driven by the promoter construct of 200E-mGluR500P (**a, b**) and In4s-In3-200En-mGluR500P (**c, d**). Retinal whole-mount (**a, c**) and vertical section (**b, d**) were co-labeled for mCherry (red; left panels) and PKC, a rod bipolar cell marker (green; middle panels). The merged images are shown in the right panels. Arrows point to the mCherry positive and PKC negative axon terminals (**b, d**).

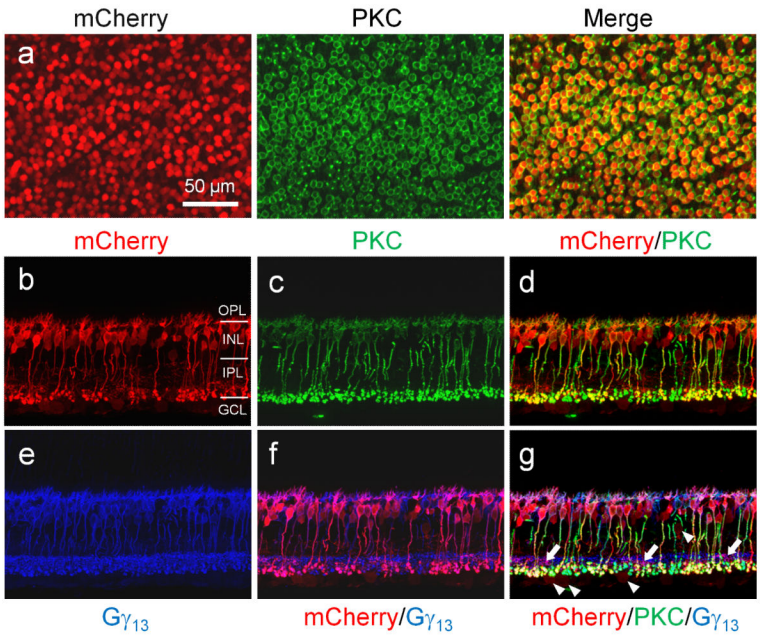

Figure 5. Immunostaining for the characterization of mCherry-expressing bipolar cells transduced by the virus vector with AAV2.7m8-Y444F capsid variant in mice

The expression of mCherry was driven by the promoter construct of In4s-In3-200En-mGluR500P. (**a**) Retinal whole-mount were co-labeled for mCherry (red; left panels) and PKC (green; middle panels). The merged images are shown in the right panels. (**b** – **g**) Triple immunolabeling in vertical sections with antibodies against mCherry (**b**), PKC (**c**), and Gγ_{13} (**e**). The merged images for mCherry/PKC (**d**), mCherry/Gγ_{13} (**f**), and mCherry/Gγ_{13}/PKC (**g**) are shown. Arrows point to the mCherry positive, PKC negative, but Gγ_{13}-positive axon terminals. Arrow heads indicate to the weakly mCherry labeled RGCs and/or amacrine cells.

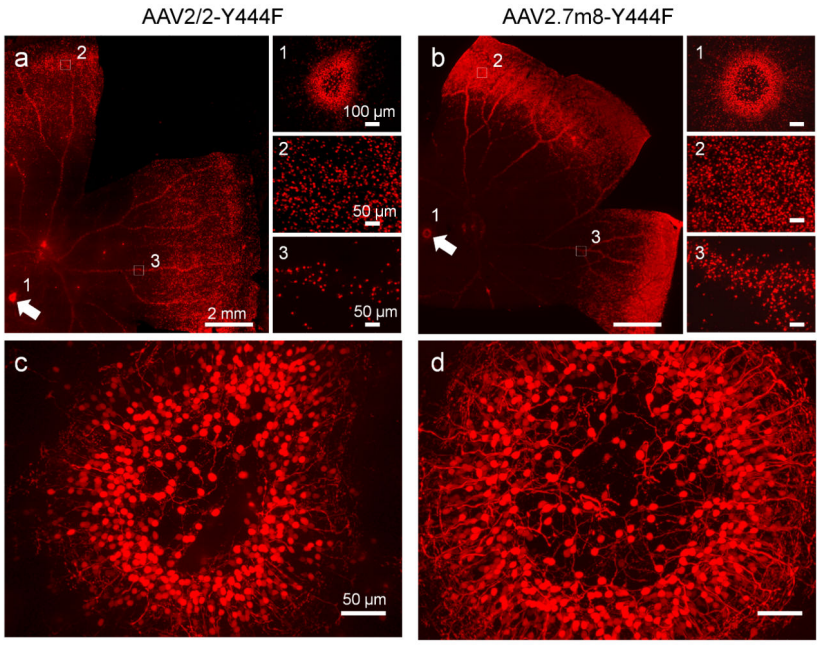

Figure 6. AAV-mediated expression patterns in the marmoset retina

The whole-mount retinas show the mCherry expression with AAV vectors driving by In4s-In3-200En-mGluR500P promoter construct with AAV2/2-Y444F mutation (**a**) and AAV2.7m8-Y444F (**b**) capsid variant, respectively. The three insertions on the right are the magnified images: (1) the fovea as indicated by arrows; (2) the representative regions of the far periphery as enclosed by dashed squares; (3) the representative regions containing blood vessels. (**c**, **d**) The higher magnification images of the fovea.

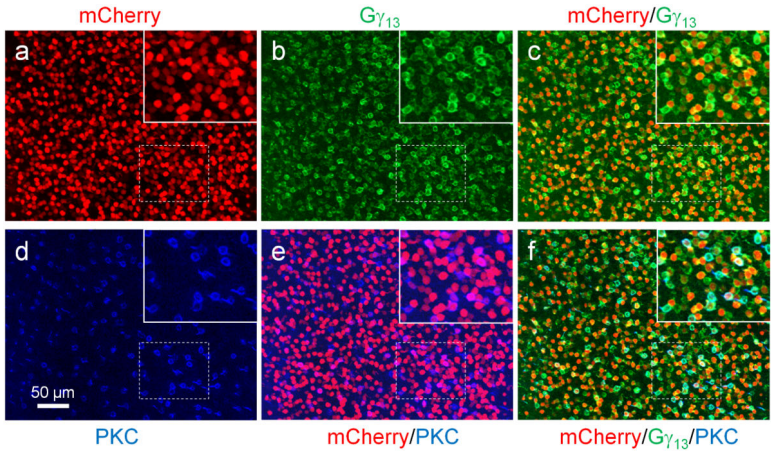

Figure 7. Immunostaining for the characterization of mCherry-expressing bipolar cells in the retinal whole-mounts of the marmoset with the virus vector carrying AAV2.7m8-Y444F capsid variant

Triple immunolabeling with antibodies against mCherry (**a**), Gγ_{13} (**b**), and PKC (**d**). The merged images for mCherry/Gγ_{13} (**c**), mCherry/PKC (**e**), and mCherry/Gγ_{13}/PKC (**f**) are shown. Inset in the upper right corner shows magnification of boxed area. The region is from the far periphery (6 – 8 mm from the fovea) of the retina.

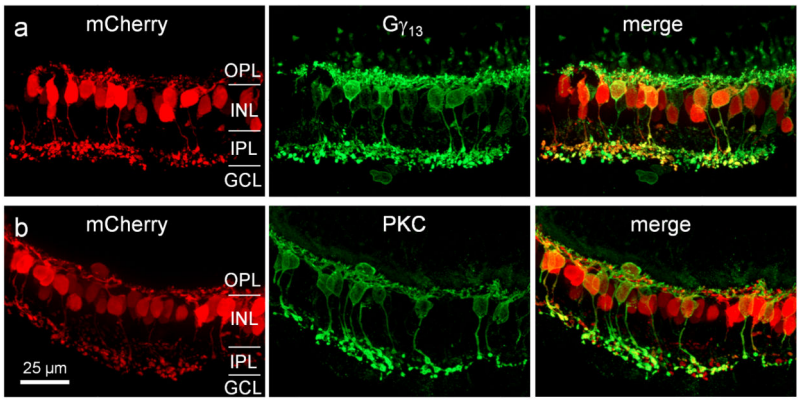

Figure 8. Immunostaining for the characterization of mCherry-expressing bipolar cells in the retinal vertical sections of the marmoset

(**a**) Double immunolabeling with antibodies against mCherry and Gγ_{13}. (**b**) Double immunolabeling with antibodies against mCherry and PKC. The merged images are shown in the right panels. The region is from the far periphery (6 – 8 mm from the fovea) of the retina transduced with the virus vector carrying AAV2.7m8-Y444F capsid variant.

Table 1

Comparison of the transduction efficiency and selectivity of virus vectors in the mouse retina.

Virus vector capsid	Promoter construct	mCherry(+) BC number/mm^2	PKC(+) BC number/mm^2	% of mCherry(+)-PKC(+)/mCherry(+)	% of mCherry(+)-PKC(+)/PKC(+)	number of retinas
AAV2/2-Y444F	200En-mGluR500P	5916 ± 985	10400 ± 685	98 ± 21	58 ± 12	4
AAV2/2-Y444F	In4s-In3-200En-mGluR500P	8952 ± 1085	10034 ± 505	92 ± 11	86 ± 7.0	3
AAV2.7m8-Y444F	In4s-In3-200En-mGluR500P	12426 ± 964	11096 ± 995	86 ± 9.0	96 ± 1.0	4

The data are presented as the mean ± SD.

Table 2

Comparison of the transduction efficiency and selectivity of virus vectors in the marmoset retina.

Virus vector capsid	Promoter Construct	mCherry(+) BC number/ mm^2	$G_{\gamma 13}$(+) BC number/ mm^2	PKC(+) BC number/ mm^2	% of mCherry(+)-$G_{\gamma 13}$(+)/mCherry(+)	% of mCherry(+)-PKC(+)/mCherry(+)	% of mCherry(+)-$G_{\gamma 13}$(+)/ $G_{\gamma 13}$(+)	% of mCherry(+)-PKC(+)/PKC(+)	number of retinas
AAV2/2-Y444F	In4s-In3-200En-mGluR500P	4340 ± 383	6137 ± 769	1567 ± 286	86 ± 3.4	18 ± 2.4	78 ± 9.3	50 ± 7.3	1
AAV2.7m8-Y444F	In4s-In3-200En-mGluR500P	5992 ± 856	6026 ± 588	1455 ± 101	95 ± 4.2	17 ± 3.1	93 ± 1.9	72 ± 5.6	1

The data are presented as the mean ± SD.